DESIGN OF THE SPORE SMALL PROBE HIGH ALTITUDE BALLOON DROP TEST

Jessica Juneau Clark[(1)] and David A. Spencer[(2)]

[(1)]Georgia Tech Student, 802 Ridge Dr. Glendale, CA 91206, USA, Email: jjuneau3@gatech.edu
[(2)]Professor of the Practice, Georgia Tech Mail Stop 0150 Atlanta, GA 30306, USA, Email: david.spencer@aerospace.gatech.edu

ABSTRACT

The Small Probes for Orbital Return of Experiments (SPORE) flight system is designed to perform atmospheric entry, descent and landing (EDL) in order to return small payloads from an Earth orbit to the ground for recovery. A high altitude balloon drop test of a nearly identical 10.51 kg re-entry probe is described. A drop altitude of 32.8km from a 0.11 mcm balloon was determined to be sufficient to test the parachute deployment system and canopy performance at flight-like dynamic pressures and Mach numbers. A Monte Carlo analysis of the drop test trajectory was performed to characterize variability of chute deployment conditions and landing ellipse size. A description of launch and ground operations is included, as well as a preliminary probe and gondola design. Finally, an overview of similar historical stratospheric balloon drop test programs is provided.

1. SPORE OVERVIEW

The Small Probes for Orbital Return of Experiments (SPORE) flight system architecture provides a scalable, modular approach to the return and recovery of multi-purpose probes from orbit. Capable of accommodating payload volumes ranging from the CubeSat 1-unit (1U) dimensions of 10x10x10 cm to 2U and 4U payloads, SPORE is targeted to carry flight experiments related to thermal protection system (TPS) performance validation, biological science, and materials science missions. SPORE is also designed to accommodate the return of small payloads from the International Space Station (ISS).

The Entry, Descent, and Landing phase for SPORE is designed to meet thermal control and g-level requirements to maintain payload health and safety. Because the desired on-orbit environment for different payloads varies dramatically, the SPORE architecture is designed to accommodate re-entry from orbits ranging from low-Earth orbit (including ISS return) and GTO. Landing sites at the Utah Test & Training Range and the Woomera Test Range in South Australia are targeted.

The EDL sequence begins when the SPORE entry vehicle is deployed from its service module following a de-orbit maneuver that targets a zero degree initial angle of attack, ballistic reentry trajectory. Peak heating and maximum deceleration are experienced during the hypersonic regime, and following the transition to subsonic flight, the cross parachute is ejected using a mortar. No jettison of the heatshield is required, as the payload is thermally isolated from the heatshield soak-back. The vehicle approaches terminal velocity on the parachute prior to touchdown, with touchdown velocities varying based upon the vehicle configuration. A UHF beacon signal will be transmitted throughout EDL to aid in the recovery process. Recovery is required to occur within two hours of touchdown.

2. HIGH ALTITUDE BALLOON DROP TEST

It is desired to increase the SPORE flight system TRL through various tasks. Of these tasks, a high altitude drop test of the entry system would provide a means of verifying flight system functionality in a near flight-like environment. High altitude balloons (HABs) provide a relatively low-cost, quick-response method for delivering the entry system to a desired altitude and releasing it, in order to test system functionality during atmospheric descent and landing. Most HAB tests can be flight-ready in as little as 6 months, and can be launched from a variety of locations because of their mobile launch platform. High altitude balloons have been used for similar drop tests on a number of NASA and ESA missions, as is detailed in Section II.

A typical test setup involves transporting the flight payload (for SPORE: the gondola and entry vehicle) to the launch pad via a crane, assembling the flight train, inflating the tethered balloon, releasing the balloon and then the payload. After the flight train reaches the desired float altitude, gondola release can be triggered from ground command, at which point the entry vehicle separates and begins to free-fall. Parachute deployment occurs autonomously, and the entry vehicle, gondola, and deflated balloon are all recovered on the ground. A more detailed description of launch and ground operations can be found in Section VIII.

For the SPORE HAB drop test, the primary objectives would be the following:

- Verify entire entry system functionality, thereby increasing the entry system TRL. This includes the communications system, command and data handling system, electrical power system, and parachute deployment system.
- Verify parachute canopy integrity at flight-like dynamic pressures and Mach numbers
- Investigate entry vehicle stability at subsonic conditions
- Gain experience with mission operations planning, hardware testing and integration, and pre- and post-flight procedures

The following sections document the initial work that has been done in designing the SPORE high altitude balloon test. This work includes surveying similar historical balloon drop programs, investigating potential HAB launch providers, and performing trade studies and Monte Carlo analyses to determine the optimal test conditions and to characterize the influence of variability on test outcomes. In addition, a preliminary description of the entry vehicle and gondola design is discussed, as well as launch and ground operations setups.

3. HISTORICAL DROP TEST PROGRAMS

High altitude balloon drop tests have long been used by NASA, ESA, and other aerospace organizations as a means of testing system functionality in a flight-like environment for relatively low cost and complexity. In order to provide a historical perspective in designing the SPORE drop test, a thorough study of similar historical balloon drop test programs was performed. Many of these programs had test objectives and flight conditions that were very similar to the SPORE drop test, and were conducted as a part of large NASA, ESA, and JAXA missions. The missions whose supporting drop tests were investigated include Galileo, Cassini-Huygens, Haybusa, Stardust, Viking, and NASA Mars subsonic parachute studies. Below is a summary of the test programs that are most applicable and useful for the SPORE drop test design.

3.1 Test Objectives

Most of the drop test programs investigated had test objectives that were similar to those of the SPORE drop test. All of them sought to, in some way, demonstrate proper parachute deployment at conditions that were as flight-like as possible. The Mars subsonic parachute tests, conducted by Mitcheltree et al.[12] in 2004 were part of an effort to develop a new parachute system for Mars exploration, and so the parachute was the primary drop test payload, whereas the larger mission tests were purposed for testing the entire entry system functionality. Both the Hayabusa MUSES-C and the Huygens probe drop tests had objectives for characterizing vehicle transonic aerodynamics and probe stability.[9,7] Observing the re-entry probe dynamics in a flight-like spin was also an objective of the Huygens probe drop tests.[9] After the initial Huygens probe drop test, an additional test was conducted to test spare sensors of the HASI (Huygens Atmospheric Structure Instrument) in dynamic conditions and to test their trajectory reconstruction algorithms.[3,4] In most of these drop test programs, the test objectives were fully met, with some exceptions where technical failures on the customer's part occurred or where the ideal flight conditions were too extreme for a low-altitude, Earth drop test.

3.2 Test Setup

The target float altitudes for the various drop test programs ranged from 29 km (Galileo) to 40 km (Viking PEPP), except for the 3.62 km Stardust drop test to test the basic entry system functionality.[18] Balloon volumes, ranging from 0.03 mcm (Hayabusa) to 0.74 mcm or million cubic meter (Viking PEPP) were used to lift suspended masses between 500 and 1500 kg.

The ascent train, or vertical chain of hardware lifted in a balloon test, can be varied from test to test, but has the same basic structure. A typical ascent train features the payload, attached to or internal to a support gondola. Above the gondola is a mechanical/electrical gondola release mechanism that is typically signaled to release via ground command. Most tests require a safety or emergency parachute above the gondola release mechanism in the event of balloon failure or for use as a means of recovering the gondola. Above the safety chute is the terminate release mechanism, which can be used to recover the support gondola (and payload, if a free fall is not desired) under the safety chute. At the top of the ascent train is the balloon, which is typically deflated upon gondola release and recovered on the ground as well. The basic ascent train can be modified, of course, to accommodate drop test needs or requirements. For the initial Huygens system drop test an auxiliary balloon was used in addition to the main Type 402 Z balloon [7], and for the later HASI test, a separate Telemetry Module (TM) was added 2.6 m above the probe and below the parachute via a heavy bifilar line.[3,4] The TM contained all instruments and supporting devices to perform probe release.[3,4] Other variations of the ascent train utilized the gondola release event to static-line deploy the drogue or main chute, as with the Stardust drop

test, Huygens HASI test, the Mars subsonic test program.[3,4,12,18]

Most of the historic drop tests featured a two-stage parachute system (drogue and main). For the Mars subsonic parachute tests, the drogue was static-line deployed after gondola release, and the time-triggered main chute was deployed with pyro cutters.[12] The Galileo probe drop tests featured a pilot chute, followed by aft heatshield removal, and then the main chute deployment. After main chute deployment, the descent module was separated from the deceleration module, as would occur during the probe's actual mission.[10,16] The Stardust systems drop test utilized the gondola separation event for static deployment of the drogue, followed by a computer-initiated main chute deployment.[18] The Huygens probe utilized a three-stage parachute system, with a pilot chute deployed at Mach 1.5, a main chute for heatshield separation, and then a stabilizer chute for the remainder of atmospheric descent. All of the Huygens drop test separation events were based on majority voting.[9] For the Huygens HASI test, a single, static-line deployed parachute was used, that was linked to the balloon via a connector pyro cable and fired via ground command. The parachute was static-line deployed, and a ballast on the TM was also jettisoned via ground command.[3,4] Both of the Hayabusa drop tests also featured a single, toroidally packed parachute (one of which was 60% reefed), that were pulled out by the parachute cover and jettisoned using pyro pushers.[7]

3.3 Gondola and Probe Design

The purpose of the gondola is to carry all support equipment for the balloon payload (be it a re-entry probe or scientific samples). It also serves as a mechanical and electrical interface between the payload and the balloon. For the Mars subsonic parachute tests, the gondola also served as the aerodynamic vehicle for the parachute system, and was released with the payload. It featured a truss structure, a faceted aerodynamic fairing, a structural base with instrumentation, and a crushable cardboard honeycomb on the nose to reduce the loading upon ground impact.[12] The gondola for the Huygens probe drop test had bracket interfaces between the probe and gondola for pyro separation, umbilical separation by a lanyard, and also featured spin vanes to generate spin rates similar to those on the actual Huygens mission.[9] For the HASI experiment, the gondola was also equipped with spin vanes, and even carried lead bricks as a mass ballast.[3]

For a majority of the drop test programs investigated, the payload was a geometrically similar (sometimes identical) mock-up of the actual re-entry probe. The probe for the Huygens drop test was a full-scale model of the actual entry vehicle, with flight-like hardware, as was the probe for the HASI experiment, with an additional ring supporting a double-plate platform, a bottom front cone, and an upper cover. For the Galileo probe drop test, a 376 kg ballast was added to the nose of the probe, increasing the vehicle's ballistic coefficient, so that flight-like dynamic pressures could be.[10] The Hayabusa MUSES-C drop test probe featured an additional antenna mounted to the forward heat shield for communication with the ground.

3.4 Instrumentation

In terms of probe and gondola instrumentation, all of the historical missions carried some form of the following: primary batteries (with Power Distribution Unit), telecommunications equipment, on-board cameras, accelerometers, pressure transducers (stagnation and internal), thermal control equipment, rate gyros, pyrotechnic devices for separation events, and data acquisition and storage equipment. Detailed descriptions of the instrumentation used on each of the historical drop tests can be found in the table in the Appendix. For primary batteries, a range of types were used including Lithium-ion (Mars subsonic chute testing, sized for 10 hour duration[12]), NiCd rechargeable batteries (Huygens probe, Hayabusa MUSES-C), and Ni-MH (for HASI experiment, sized for 8 hour duration).[3] Most telecommunication systems featured ground-to-gondola uplink and downlink, but the Huygens probe featured a L-band gondola-to-ground link, an S-band probe-to-gondola link, and an S-band probe-to-ground link for data backup. Most of the missions carried CCD or film cameras for monitoring parachute deployment and separation events. The Mars subsonic parachute test carried 2 up-looking mini-digital-video camcorders, 1 up-looking camera connected to telecoms for ground storage, an additional down-looking camera, 1 chase plane camera, and one ground telescope camera.[12] For altitude (and latitude/longitude) knowledge, some drop test probes carried on-board GPS's (Mars subsonic chute test, HASI test, and Huygens probe drop test). The Huygens probe drop test also used differential GPS between the probe and gondola.[9] For the Hayabusa drop tests, the altitude was estimated using pressure transducer data and camera data. Most of the drop tests carried 1-axis or 3-axis accelerometers, and 2-axis rate sensors. The Mars subsonic chute test also carried a Northrup Grumman LN-200 IMU, with 3-axis rate gyros and 3-axis accelerometers.[12]

Information regarding the testing objectives, test setups, and probe/gondola instrumentation for similar historical missions provided invaluable references used to aid in the design of the SPORE drop test.

4. TEST CONFIGURATION TRADE STUDY

In order to design a high-altitude balloon drop test of the SPORE entry system, a trade study was performed to select the desired test setup and conditions. This analysis was used to determine parameters such as the necessary balloon volume, float altitude, system mass, and parachute deployment timer settings. The tool used for the subsequent trade studies involved a three degree-of-freedom (3-DOF) trajectory simulation, a parachute drag and inflation model, an aeroshell drag model, a standard atmosphere model, and an atmospheric winds model, all of which are described in the following sections.

4.1 3-DOF Trajectory Simulation

A 3-DOF simulation of drop test probe and parachute trajectory was written, that includes non-planar and rotation effects. Normal forces on the vehicle (due to lift) were neglected in the kinematic and force equations because the body was assumed to always be at 0^o angle of attack. By numerically integrating these equations using a small time step (0.1 seconds) one can estimate the trajectory of the drop test vehicle with a computation time that is reasonable for Monte Carlo analyses.

4.2 Parachute Model

The main parachute for the SPORE entry vehicle is a mortar-deployed, cross-type parachute manufactured by Pioneer Aerospace, for use on 16kg flares. It provides enough drag force to decelerate the vehicle to a required 5 m/s touchdown velocity to avoid damage to the thermal protection system. The chute has a nominal diameter of 4.5 m and a nominal drag coefficient of 0.675. A side view of a typical cross parachute can be seen in Fig. 1 below.

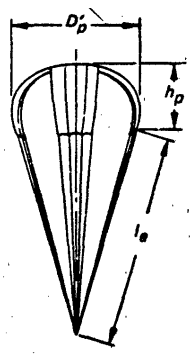

Fig. 1. Inflated profile of cross-type parachute.[1]

For the test condition trade study and Monte Carlo analyses, several assumptions were made regarding the parachute, because of limited information. The combined length of the bridles, suspension lines, and riser was assumed to be 5 nominal diameters (as is typically with subsonic, cross-type parachutes). In addition, the mortar ejection force was assumed to be 10 N and was assumed to provide a 10 m/s relative ejection velocity.

Because parachute inflation for SPORE takes place in a dense atmosphere with a light vehicle, significant deceleration will occur during inflation, and so it cannot be assumed to be an infinite mass process. A standard model for parachute inflation is the Pflanz inflation model, which was used for the SPORE drop test parachute.[1] Equation 1 below shows the Pflanz relationship between parachute force (F_P) and various parachute characteristics, including the nominal chute drag area ($C_{Do}S_o$), the opening force factor (C_X), the canopy fill constant (n), time of line stretch (t_{LS}) and the time of full chute inflation (t_{FI}).

$$F_P(t) = q(C_{Do}S_o)C_X\left(\frac{t - t_{LS}}{t_{FI} - t_{LS}}\right)^n \quad (1)[1]$$

The opening force factor accounts for the overshoot in drag force experienced by most parachute inflation processes, whereas the canopy fill constant gives the correct shape to the inflation profile and is based on empirical relationships. Both are a function of canopy type, and for an infinite mass inflation scenario, both can be assumed to be constant. However, because the drop test inflation would be better approximated as a finite mass inflation, C_X was assumed to vary as a function of the parachute canopy loading factor, or the vehicle weight over the parachute drag area ($m_{vehicle}\, g / C_{Do}S_o$). For the SPORE drop test article, the canopy loading factor is around 9.6 N/m^2, and using a relationship from Knacke et al.[1], the opening force factor reduction is nearly 95%! Therefore, a value of 0.1 was used for C_X and 11.7 was used for n (both based on empirical data from Knacke et al.[1] for cross-type parachutes). The values for time of line stretch (t_{LS}) and time of full inflation (t_{FI}) were found using Equations 2 and 3 shown below.

$$t_{LS} = \frac{l_{lines}}{V_{eject}}\ ,\ t_{FI} = \frac{nD_o}{V_{LS}} \quad (2)\ (3)[1]$$

Here l_{lines} is the combined length of the bridle, riser, and suspension lines, V_{eject} is the relative parachute ejection velocity, D_o is the nominal parachute diameter, and V_{LS} is the vehicle velocity at line stretch.

4.3 Aeroshell Drag Model

The geometry for the SPORE re-entry probe was taken from the Mars Microprobe geometry, featuring a 45-degree spherecone with a hemispherical afterbody whose radius of curvature is centered at the vehicle's center of gravity (for forward-reorienting stability

purposes, see Mitcheltree et. al[13]). The geometric relationships for this aeroshell are shown in Fig. 2.

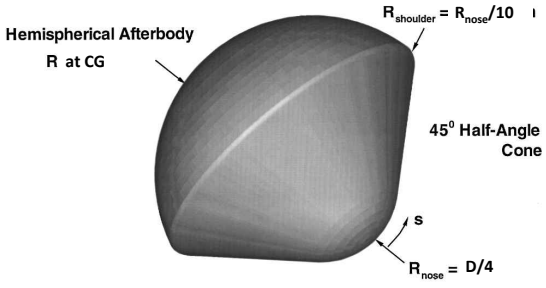

Fig. 2. SPORE Re-entry Probe Geometry (Mars Microprobe)[13]

A drag profile for the entry vehicle was constructed using the various wind tunnel and CFD data used in similar analyses for the Mars Microprobes.[13] The drag models included in the POST program for a forty-five degree spherecone were also used to construct the SPORE drag model. Fig. 3 shows a plot of the SPORE drag model, along with wind tunnel data, CFD LAURA data, and the Newtonian flow solution for hypersonic velocities.

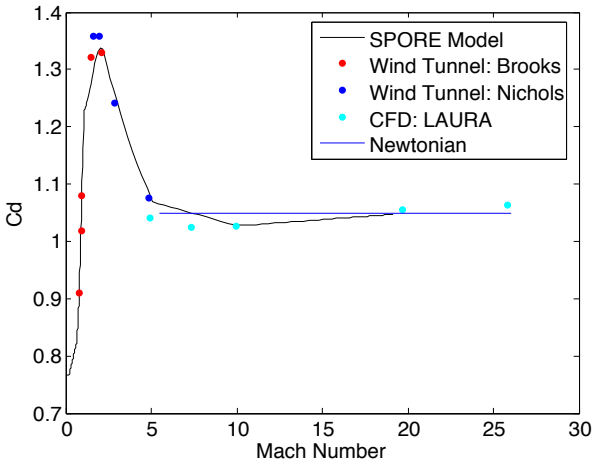

Fig. 3. Drag Profile for 45° Spherecone.[13]

For Mach numbers above 20, the drag coefficient was assumed to be constant at 1.048. This drag model was then used for both the test condition trade study and Monte Carlo analyses of the drop test.

4.4 Atmospheric Winds Model

In both the trade studies and Monte Carlo analyses, atmospheric winds were included in the vehicle's Earth-relative velocity. A winds model was taken from Hedlin et al.[6] for mesospheric and stratospheric winds at 30 to 60°N latitudes (assuming a launch out of New Mexico or Texas). The wind speed as a function of altitude can be seen in Fig. 4. As will be explained in the Monte Carlo Uncertainty Characterization section, an uncertainty (and therefore 6-sigma offset) of 10 m/s was assumed for the winds profile, because all of the drop test conditions occur in the stratosphere.

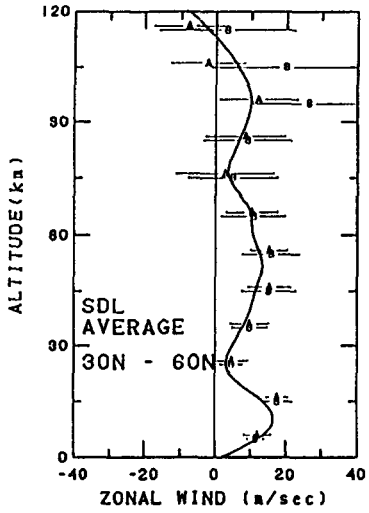

Fig. 4. Empirical Atmospheric Winds Profile for 30 to 60°N.[6]

To include the effects of wind speed on the vehicle's relative velocity, the wind speed component for a given altitude was simply included in the horizontal vehicle velocity. The winds, zonal and meridional, were assumed to be strictly horizontal to simplify the simulations. Equation 4 shows the Earth-relative vehicle velocity, updated to include winds, where V is the vehicle velocity before winds and Vwinds is the estimated wind speed.

$$V_{total} = \sqrt{\left(V_{winds} + V\cos\gamma\right)^2 + \left(V\sin\gamma\right)^2} \qquad (4)$$

4.5 Defining Test Parachute Deploy Conditions

The drop test was designed to provide flight-like dynamic pressures and Mach numbers at parachute deploy in order to verify parachute and parachute system functionality. The nominal LEO return trajectory for a SPORE TPS testbed mission has the entry state characteristics shown in Table I below, with the values for initial velocity, altitude, flight path angle, latitude, longitude, heading angle, and mass all listed respectively.

Table I: SPORE LEO, TPS Testbed Nominal Entry State

Parameter	Value	Units
V_o	7780	m/s
h_o	125	km
γ_o	-5.0	°

ϕ_o	137.65	°E
θ_o	-16.65	°N
ψ_o	267.10	°
m_o	10.51	kg

For this trajectory, the main parachute is deployed subsonically at a desired deployment Mach number of 0.8, which will be targeted using a timer and a G-switch. At this deployment condition, the approximate dynamic pressure is 1.0088 kPa. An altitude versus velocity plot of this nominal LEO trajectory is shown in Fig. 5 below, with a callout for parachute deploy.

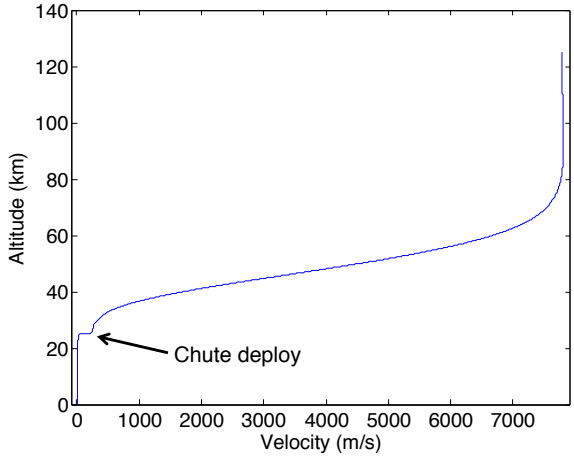

Fig. 5. SPORE Nominal LEO TPS Testbed Trajectory.

4.6 Defining The Drop Test Conditions

A trade study was performed on drop test initial conditions in order to achieve flight-similar dynamic pressures and Mach numbers at parachute deployment. By varying balloon float altitude (which is a function of suspended mass), the potential energy of the drop test system can be varied to achieve different test conditions. The standard NASA relationship between float altitude and suspended weight used for a 0.11 mcm volume balloon. The 0.11 mcm balloon turned out to provide sufficient altitude to meet test conditions and was also ideal because drop test cost is typically a function of balloon volume.

To find the best drop test conditions, balloon float altitude was varied from 37.5 km to 29 km, for both a scenario with winds and without winds, to compare the differences. For the no-winds scenario, the optimal suspended mass was 577 kg, which can achieve a float altitude of 33.62 km with a 0.11 mcm balloon. This initial condition reaches a dynamic pressure of 1.0101 kPa at a Mach number of 0.8115 at 45.3 seconds after separation from the gondola. A plot of the dynamic pressure and Mach number for varying float altitudes is shown in Fig. 6, with the best-fit trajectory highlighted in cyan and the parachute deployment condition shown with a red marker.

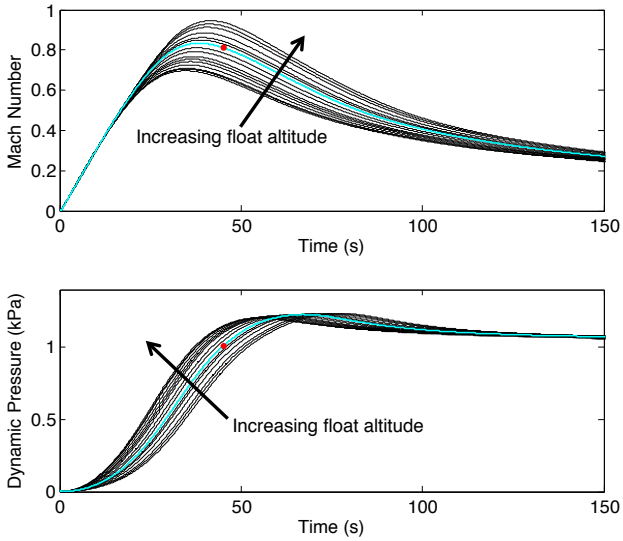

Fig. 6. Sweep of float altitude for 0.11 mcm balloon. (Desired chute deployment condition highlighted in red on cyan trajectory.)

However, with winds included in the trade study, the best-fit test condition is slightly different. The best balloon float altitude is at 32.821 km, requiring a suspended mass of 726.09 kg. With this initial altitude, the vehicle reaches a parachute deployment condition 43 seconds after gondola separation, with a dynamic pressure of 1.0045 kPa and a Mach number of 0.7979, as shown in Fig. 7. With the addition of the winds into the trajectory simulation, the dynamic pressures experienced by the vehicle are higher during the lower-altitude portions of the trajectory, rather than at the higher velocity segments at higher altitudes.

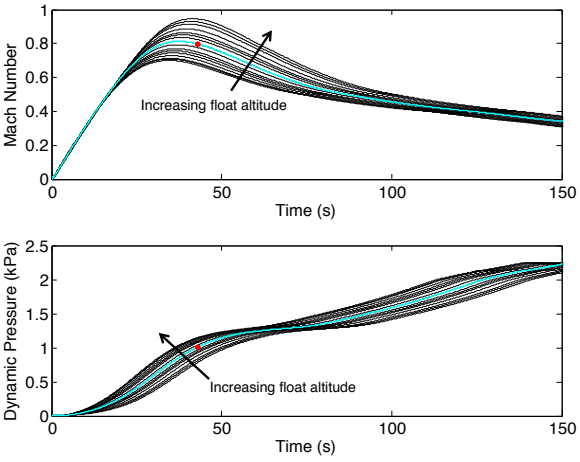

Fig. 7. Sweep of float altitude for 0.11 mcm balloon (with winds).

Because including winds in the model was found to cause significant differences in the initial test conditions, the second test condition (at 32.8 km float altitude) was assumed for the actual drop test.

5. MONTE CARLO ANALYSIS

In order to investigate the effects of various test conditions on parameters such as parachute deployment conditions and landing footprint, a Monte Carlo analysis was performed for the SPORE drop test. Large amounts of output and input data were needed, and so 500 cases were selected to save on memory but also capture the final distributions of the various outputs.

5.1 Uncertainty Characterization

To account for the uncertainties associated with many of the test parameters, distributions of values were assumed for the Monte Carlo analysis.

Table III in the Appendix details the distributions assumed for each parameter, along with their mean value and standard deviation (for normal distributions) or upper and lower bounds (for uniform distributions).

For several of the parameters, the standard deviations were selected such that the 6-sigma values were within the estimated upper and lower bounds. For ho an uncertainty in the float altitude of +/- 100 m was assumed, whereas for the nominal parachute diameter (Do) an uncertainty of +/- 5 cm was assumed. The parachute drag coefficient was given as a range from 0.65 to 0.70, and so a mean value of 0.675 with a 6-sigma offset of 0.025 was assumed. The time of parachute deploy was assumed to potentially occur ½ a second before or after the desired time, to account for inaccuracies in the timer. Because the parachute snatch force varies with deployment dynamic pressure, it was assumed to have a 10%, or 300 N variation about the mean. The mortar ejection force was assumed to vary by 50% and the ejection velocity, by 25%, because of a lack of information regarding the mortar capabilities. Because the probe mass has not been fully characterized, a mean value of 10.51 kg was used to match the actual SPORE vehicle mass, with a 10% variation.

The initial heading angle, ψ_o, was assumed to have a uniform distribution from 0^o to 360^o, because the drop test initiates in a nearly-vertical configuration, and so depending on the zonal and meridional winds, the probe could potentially have a heading angle in any direction. This initial heading angle, however, doesn't have much of an effect on the test outcomes, because the initial flight path angle is 90^o to within ½ a degree.

As mentioned in the Test Configuration Trade Study section, an atmospheric winds model was taken from Hedlin et al. for zonal and meridional winds at 30 to 60^oN latitudes. Hedlin characterized the overall root mean square differences between all of the data used to create his model as being on the order to 15 m/s in the mesosphere (85km to 50km altitudes) and 10m/s in the stratosphere (50km or less).[6] Because all drops investigated occurred at less than 50km, the stratospheric RMS value of 10m/s was used as the 6-sigma value for the wind speed distribution.

The driving factor for variations in initial latitude and longitude is balloon drift, which can be quite significant for high altitude balloon tests. In order to characterize the bounds on balloon drift, values of observed drift were taken from similar historical tests. For example, for the Huygens HASI Balloon Drop Test, the balloon drifted within a radius of 50km during the whole of ascent, float, and descent. Fig. 8 shows the drift profile measured during the HASI drop test. This test had a float altitude of approximately 32 km (close to the SPORE target float altitude) and took place over a period of 3.6 hours.[3] Similarly, the Viking PEPP parachute drop tests observed a maximum balloon drift of 39.3 km (See Fig. 9**)** for tests performed at White Sands, New Mexico with a 39 km target float altitude.[15] Based on these two historical observations, a max drift radius of 50km was assumed (as a worst-case scenario), which is equivalent to a 0.45 degree change in latitude and longitude. This 0.45 degrees was used as the 6-sigma offset for the Monte Carlo initial latitude and longitude values. The mean values were assumed to be the location of the CSBF facility in Palestine, Texas.

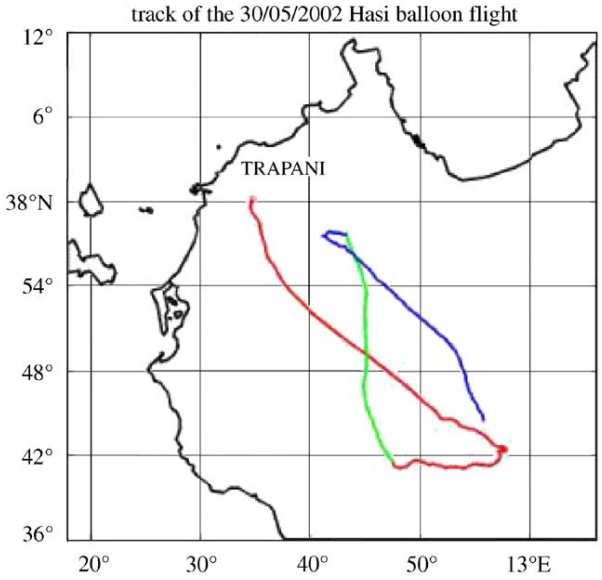

Fig. 8. Balloon drift profile for Huygens HASI drop [3]. Red = ascending, green = float, blue = descending

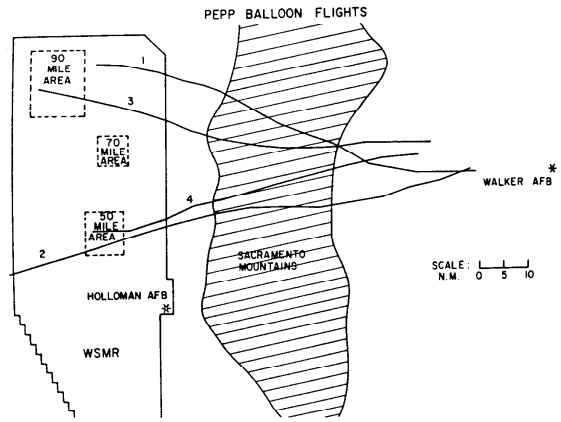

Fig. 9. Viking PEPP balloon drift profiles.[15]

5.2 Results

Using the distributions listed in

Table III**,** a 500-case Monte Carlo analysis was performed. As expected, the variability in the initial conditions resulted in variability of the vehicle trajectory and parachute deployment conditions. In Fig. 10, the vehicle altitude versus velocity is plotted for all 500 cases. One can see that the horizontal "band" at which the vehicle decelerates from parachute inflation covers approximately 2.5 km, so there is significant variety in parachute deployment altitude.

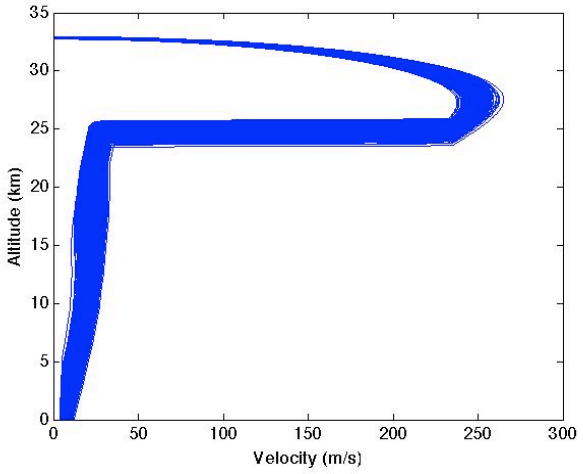

Fig. 10. Altitude vs. Velocity for Full Swath of Monte Carlo Trajectories.

To capture the variability in parachute deployment conditions, histograms of the dynamic pressure, altitude, and Mach number at mortar fire were generated, as can be seen in Fig. 11. The dynamic pressure distribution captured the desired condition (1008 Pa), and ranged from values of 894 Pa to 1323 Pa and was skewed to the lower values. The altitude of mortar fire ranged from 24.2 km to 26.4 km and was skewed to the high altitudes. Finally, the Mach number at mortar fire ranged from 0.7737 to 0.8307, and is centered around the target value of 0.8.

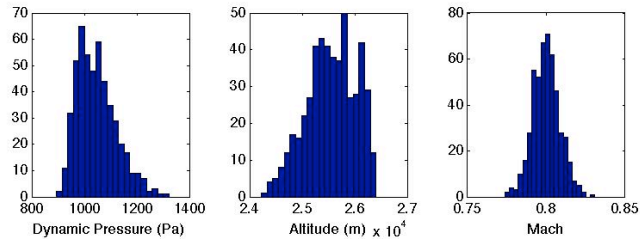

Fig. 11. Parachute Deployment Conditions (Distributions).

Fig. 12 shows the correlation between the Mach number and dynamic pressure at mortar fire for each of the 500 cases. The desired condition is highlighted in red. As one can see, the scatter is relatively centered about the target value, with minimal spread on the deployment Mach number (approximately +/- 3%). There is larger variability associated with the deployment dynamic pressure, ranging up to 31% higher than the target value. This is something that could be adjusted with a more accurate mortar timer or better control over float altitude. However, because most of the off-nominal cases are at larger dynamic pressures (i.e. more stressful conditions for the canopy), one would be more certain of parachute functionality for the actual SPORE deployment conditions.

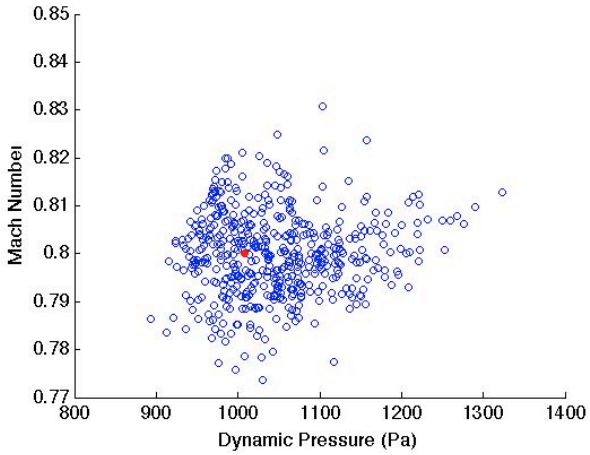

Fig. 12. Scatter of Mach Number and Dynamic Pressure at Chute Deployment. Target Value Highlighted in Red.

The final goal of the Monte Carlo analysis was to characterize the drop test vehicle landing ellipse. Because the vehicle is Earth-facing at gondola release (-90^{o} flight path angle), the largest driving factor of landing ellipse size is the initial latitude and longitude distribution because of balloon drift. A scatter of the latitude and longitude of the vehicle at touchdown is

shown in Fig. 13, with the mean value highlighted in red. Taking the extremes of both latitude and longitude yields a landing ellipse of 108.26 km North-South and 111.79 km East-West. This ellipse would be acceptable for a CSBF launch out of Palestine, Texas and would fall within their 200-mile payload drop-radius requirement.[2]

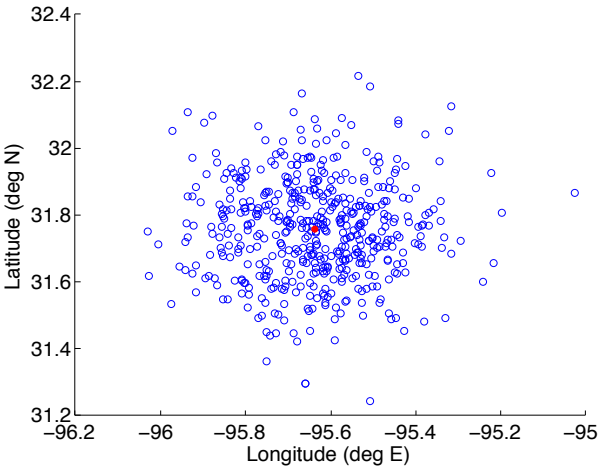

Fig. 13. EDL Landing Ellipse, Center Highlighted in Red.

6. TEST VEHICLE DESIGN

6.1 Entry Capsule Design

The entry probe for the SPORE drop test would be very similar to the actual 1-U SPORE vehicle in terms of mass, geometry, and hardware. The SPORE 1-U entry vehicle has a max diameter of 16 inches (to provide 1:1 geometric similitude with TPS arcjet testing models), and has a current best estimated mass of 10.51 kg. Using hardware that is as similar to flight hardware as possible would be desired in order to demonstrate the system functionality. Of course, additional instrumentation would be needed to provide test-specific data. The original 1-U SPORE packaging model features the 45-degree spherecone base structure covered in the forebody and aftbody TPS. Internal to the structure is a circular shelf onto which all electronics and hardware are mounted. The parachute, packaged in the mortar takes up the largest internal volume and would extend through a central cut-out in the shelf. At the nose of the vehicle is an aluminum ballast that also serves as a heat sink to protect the electronics. Attached to the top of the shelf would be all of the internal electronics: the batteries, PDU, comms antenna and receiver, and data processing and storage devices. These are all of the hardware currently included in the SPORE 1-U packaging model.

In addition to the standard hardware, the drop test probe would feature an up-looking camera, mounted to the aftbody structure and protruding slightly through the aftbody TPS. This would be offset from the vehicle centerline to avoid the parachute mortar cap during parachute deployment. The camera would provide video footage of the parachute deployment, inflation, and dynamical behavior throughout the process. For the mass budget, the Allied Pike F-100 CCD camera was used as a placeholder (this camera could be a viable option, as it provides outstanding image quality and high frame rates). In order to back out the probe's dynamical behavior during the drop test, a 3-axis accelerometer and 3-axis rate gyro would also be used. As a placeholder, the Arduino 3-axis accelerometer (ADXL-345) and their triple-axis digital output gyro (ITG-3200 Breakout) were used in the mass budget. These two chips are extremely lightweight (<2mg) and would provide digital output to be interfaced with the processor. To monitor hardware temperatures, several thermocouples would also be integrated into the drop test probe, and to determine the freestream stagnation, static, and dynamic pressures, a differential pressure transduces would be mounted to the vehicle nose, protruding through the forebody TPS. For the mass budget, the Omega PXM409-350HGV differential pressure transducer was used as a placeholder. Finally, as an option for vehicle altitude, latitude, and longitude knowledge, a GPS receiver and antenna could also be included in the drop test probe. The Surrey Satellite Technology SGR05 GPS receiver and antenna were used in the mass budget. A preliminary cross-sectional view of the drop test probe packaging can be seen in Fig. 14, with callouts to major hardware. In addition, a preliminary mass budget of the drop test probe was developed and is shown in Table II. As one can see, the total system mass is very similar to the actual entry vehicle mass of 10.51kg.

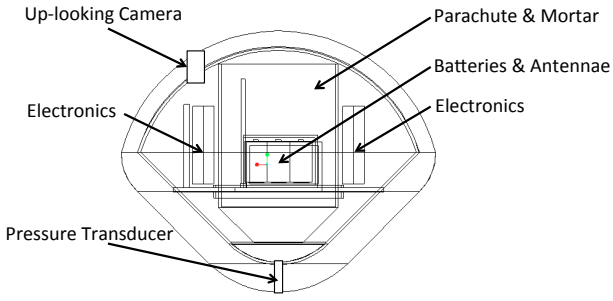

Fig. 14. Preliminary Drop Test Probe Packaging Model.

Table II. Approximate Mass Budget for Drop Test Entry Probe.

Component	CBE (kg)
Forebody Structure	0.960
Aftbody Structure	1.080
Forebody TPS	1.200
Aftbody TPS	0.400
Component Shelf	0.540
Primary Batteries (3)	0.260
Power Control Board/Battery Mounting	0.450
Camera	0.250
3-Axis Accelerometer & Casing	0.015
Differential Pressure Transducer	0.200
Temperature Sensors	0.020
Triple Axis Rate Gyro & Casing	0.018
Processor (with Flash Memory)	0.650
Antennae	0.220
Comms Transmitter	0.310
GPS	0.020
Parachute & Canister	1.440
Mortar	1.470
Heatsink/Ballast	1.010
Total Mass	**10.513**

6.2 Gondola Design

The purpose of the drop test gondola is to provide a mechanical and electrical interface between the probe and the rest of the ascent train. The gondola also carries all additional instrumentation and hardware not internal to the probe, and can provide an additional communications link between both the ground and the probe. For the SPORE drop test, a relatively simple gondola design would be required. A drawing of a gondola concept for the SPORE drop test can be seen in Fig. 15. The gondola structure could be a simple truss structure with a hexagonal shelf for mounting all hardware. At the gondola base, a series of support bars would mechanically attach to the outer diameter of the drop test probe. Upon ground command, a series of pyrotechnic bolts would fire, detaching the probe from the gondola. At the top of the gondola structure there would be a mechanical attachment to the suspension cables that are then connected to the rest of the ascent train.

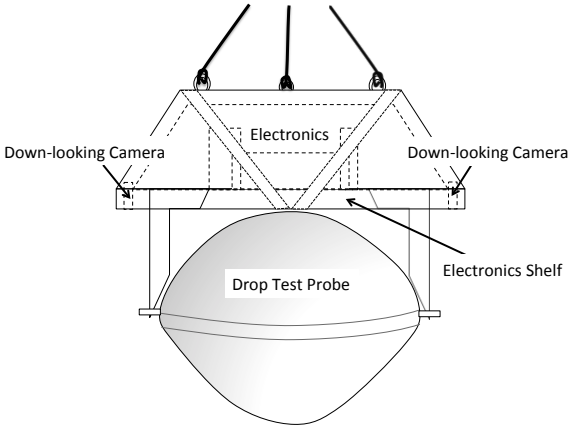

Fig. 15. Preliminary SPORE Drop Test Gondola Design.

In terms of hardware, the gondola could have a single or multiple down-looking cameras to provide footage of probe separation. The gondola could also carry a GPS receiver and antenna, to provide differential GPS capability with the probe during its descent. Data storage and handling devices could also be mounted to the gondola shelf, along with the launch provider CIP, an electronics interface which provides a ground-to-balloon telemetry link for transmitting command, tracking, and telemetry signals to and from the payload.

7. GROUND AND LAUNCH OPERATIONS

An overview of basic pre-flight, launch, ascent, descent, recovery, and post-flight operations are described in the proceeding sections. This information largely comes from the CSBF *Conventional Balloon Flight Support: Balloon Flight Application Procedures User Handbook*[2], but is relatively standard for all high altitude balloon launch providers.

7.1 Pre-Flight Activities

Before a high altitude balloon test is considered flight-ready, the test program must undergo a variety of inspections, certifications, and meetings. In the early stages of test program development, the science group (or customer) holds a Flight Requirements Meeting with the launch provider staff to review the mission's minimum success criteria, in order to set forth the facilities requirements and maintain that minimum success is realistic. Under the CSBF process, the customer is then provider a CIP (electronics interface), which provides a ground-to-balloon telemetry link for transmitting command, tracking, and telemetry signals to and from the payload. Next, the customer undergoes a Gondola Design Certification, ensuring that the gondola adheres to all FAA and NASA Safety standards, as well as launch provider gondola structural, thermal, fastener, and pressure vessel

requirements. If radioactive materials are present in the payload, a Radioactive Material Inspection is held to monitor radioactive sources and acquire a Nuclear Launch Safety Approval from the NASA Balloon Program Office.[2]

After the payload is integrated with the CIP, the launch provider electronics personnel perform an Interface Compatibility Check of the electronics interfaces. The Flight Operations personnel also conduct a Rigging Equipment Check, in which all ascent train equipment are selected, pull-tested, and certified as flight-ready. Meteorological activity is monitored daily in order to identify balloon launch opportunities, and after flight-readiness, daily Flight Status Meetings are held to review launch priority, flight opportunities, and weather forecasts. Once the flight system is considered flight-ready and a launch date is set, the gondola final weight is taken with the PI's sign-off. No more than 72 hours prior to launch, a Flight Readiness Review is held, in which the entire flight train's mechanical and electrical compatibility is certified and flight profile is confirmed. The launch window is defined, as well as the gondola and payload recovery operations.[2]

7.2 Launch and Flight Activities

On the day of launch, the Campaign Meteorologists use current and predicted weather conditions to estimate the launch window. The launch support personnel then pick up the balloon payload using a mobile launch vehicle, shown in Fig. 16, and the customer and launch personnel perform a check of all electronic interfaces in the staging area. After checkout, the mobile launch vehicle carries the payload to the launch pad, and all remaining flight line checkouts and payload preparations are performed.[2]

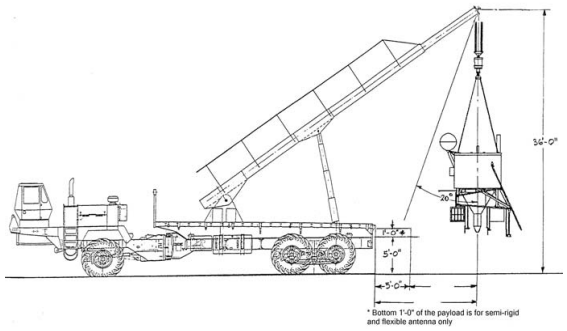

Fig. 16. Mobile Launch Vehicle.[2]

If weather conditions hold, the flight train is assembled and checked out on a protective ground cloth. The flight train equipment and parachute are laid out, and the parachute stream is checked for any damage. The balloon is laid out next and attached to the parachute and the spool vehicle (See Fig. 17). After the ascent train is fully checked out, balloon inflation begins. A pre-calculated amount of helium is pumped into the balloon through helium valves (not fully inflating, to allow room for expansion during atmospheric rise). After inflation, the balloon is released from the spool vehicle and the payload is maneuvered perpendicularly below it. After the balloon is directly above the payload and Mobile Launch Vehicle, the payload is released and begins its ascent to the desired float altitude, thus concluding the balloon launch. A concept for the SPORE ascent train can be seen in Fig. 18.

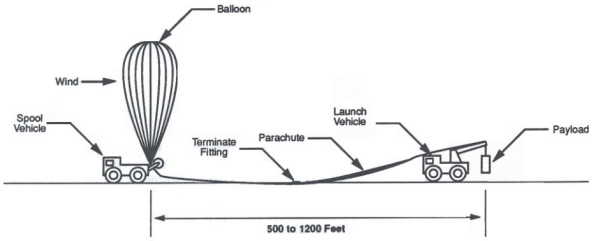

Fig. 17. Flight Train and Balloon Layout.[2]

Data collection and command control is maintained from pre-launch until payload recovery. After the float altitude is reached, the probe is separated from the support gondola via ground control. After the probe has been safely separated, the parachute recovery system deploys upon ground command, deflating the balloon and carrying the gondola to the ground for recovery. The gondola, balloon carcass, and probe are all recovered by the ground crew, returning the probe to the customer. After completion of the balloon flight, the PI fills out a post-flight assessment form before leaving the launch site, and the customer receives all downlinked and stored data relevant to their science mission.

Fig. 18. Concept for SPORE Drop Test Ascent Train (Not to Scale).

8. CONCLUSIONS

In conclusion, a high altitude balloon drop test of the SPORE Earth entry vehicle was presented as a means of testing parachute functionality at flight-like conditions, re-entry dynamics and stability, as well as entry system functionality. The final drop test probe mass was estimated to be 10.51 kg, and would require a drop from 32.8 km altitude from a 0.11 mcm balloon in order to achieve flight-like dynamic pressure and Mach number at parachute deploy, based on a trade study of varying float altitudes and balloon volumes. The landing ellipse size and variability of parachute deployment conditions were characterized using a Monte Carlo analysis on the drop test trajectory. In addition, a preliminary gondola and probe design were described, as well as a description of standard pre-flight and flight procedures for high altitude balloons. As a helpful reference, data was also gathered from similar historical drop test programs and is included, as it greatly influenced the SPORE drop test design.

9. REFERENCES

1. Bixby, H. W., Ewing, E. G., and Knacke, T. W., *Recovery Systems Design Guide*, AFFDL-TR-78-151, 1978.

2. C*onventional Balloon Flight Support: Balloon Flight Application Procedures User Handbook*, Columbia Scientific Balloon Facility, OF-600-10-H. 1 May 2006, pp. 1-40.

3. Fulchignoni, M., Aboudan, A. , Angrilli, F., Antonello, M., Bastianello, S. , et al. (2004). "A Stratospheric Balloon Experiment to Test the Huygens Atmospheric Structure Instrument (HASI)," *Planetary and Space Science*, Vol. 52, No. 9, pp. 867-880.

4. Gaborit, V., Antonello, M., and Colombatti, G., "Huygens Structure Atmospheric Instrument 2002 Balloon Campaign: Probe-Parachute System Attitude Analysis," *Journal of Aircraft*, Vol. 42, No. 1, Jan 2005, pp. 158-165.

5. Givens, J. J., Nolte, L. J., Pochettino, L. R.. (1983). "Galileo Atmospheric Entry Probe System: Design, Development, and Test," *21st AIAA Aerospace Sciences Meeting*; Reno, NV; 10-13 Jan., p. 1-18.

6. Hedlin, A. E., Fleming, E. L., Manson, A. H., et al. (1996). "Empirical Wind Model for the Upper, Middle, and Lower Atmosphere," *Journal of Atmospheric and Terrestrial Physics*, Vol. 58, No. 13, pp. 1421-1447.

7. Hinada, M., Ishii, N. , Hiraki, K. , & Inatani, Y. (1999). "Recovery System of MUSES-C Reentry Capsule," *ESA Symposium on European Rocket and Balloon Programmes and Related Research,* 14th, Potsdam, Germany; May 31-June 3 1999, 89.

8. Inatani, Y., Ishii, N. , Hiraki, K. , Hinada, M. , Nakajima, T., et al. (1997). "Parachute Deployment Experiment for a Small Capsule Dropped from a Balloon," *AIAA, Aerodynamic Decelerator Systems Technology Conference and Seminar, 14th,* San Francisco, CA; 3-5 June 1997, p. 3-5.

9. Jakel, E., Rideau, P. R., Nugteren, P. R., Underwood, J., Faucon, P., Lebreton, J-P. (1998). "Drop Test of the Huygens Probe from a Stratospheric Balloon," *Adv. Space Res.*, Vol. 21, No. 7, pp. 1033-1039.

10. McMenamin, H. J. and Pochettino, L. R. (1984). "Galileo Parachute System Modification Program." *8th AIAA Aerodynamic Decelerator and Balloon Technology Conference*; Hyannis, MA; 2-4 April., p. 2-11.

11. Meltzer, M., *Mission to Jupiter: A History of the Galileo Project*, 1st ed., NASA Office of External Relations: NASA History Division, Washington, DC, 2007, Chap. 2.

12. Mitcheltree, R., Bruno, R. , Slimko, E. , Baffes, C. , Konefat, E. , et al. (2005). "High Altitude Test Program for a Mars Subsonic Parachute". *18th AIAA Aerodynamic Decelerator Systems Technology Conference and Seminar;* Munich; Germany; 23-26 May 2005, p. 1-11.

13. Mitcheltree, R.A., Moss, J.N., Cheatwood, F.M., Greene, F.A., and Braun, R.D., "Aerodynamics of the Mars Microprobe Entry Vehicles," AIAA Paper 97-3658, *Atmospheric Flight Mechanics Conference*, New Orleans, LA, August 11-13, 1997.

14. *NSC: Near Space Corporation*. Near Space Corporation, 2011. Web. 21 Mar. 2012. <http://www.nsc.aero>.

15. Payne, J. (1967). "Balloon Development for the Planetary Entry Parachute Program (Initial Balloon Design Considerations for Planetary Entry Parachute Program)," *Its Proc., 4th Afcrl Sci. Balloon Symp*, 11.

16. Rodier, R.W., Thuss, R., Terhune, J.E., (1981). "Parachute Design for the Galileo Jupiter Entry Probe." *7th AIAA Aerodynamic Decelerator and Balloon Technology Conference*; San Diego, CA; 21-23 Oct., pp. 1-9.

17. Vinh, N., Busemann, A., and Culp, R. D., *Hypersonic and Planetary Entry Flight Mechanics*, University of Michigan Press, 1980.

18. Witkowski, A. (1999). "The Stardust Sample Return Capsule Parachute Recovery System," *CEAS/AIAA Aerodynamic Decelerator Systems Technology Conference, 15th,* Toulouse, France; 8-11 June 1999, pp. 308-315.

APPENDIX:

Table III. Parameter Uncertainties for Monte Carlo Analysis.

Parameter	Description	Units	Distribution Type	Mean Value	Standard Deviation	Upper Bound	Lower Bound
h_o	Float altitude	km	Normal	32.82	0.033	N.A.	N.A.
ϕ_o	Drop latitude	^{o}N	Normal	31.76	0.15	N.A.	N.A.
θ_o	Drop longitude	^{o}E	Normal	-95.63	0.15	N.A.	N.A.
ψ_o	Initial heading	deg	Uniform	N.A.	N.A.	0	360
D_o	Nominal chute diam.	m	Normal	4.5	0.0167	N.A.	N.A.
C_{Do}	Chute drag coefficient	--	Normal	0.675	0.0083	N.A.	N.A.
t_d	Time to chute deploy	s	Normal	40.9	0.1667	N.A.	N.A.
F_S	Snatch force	N	Normal	3000	100	N.A.	N.A.
F_{eject}	Mortar ejection force	N	Normal	10	1.667	N.A.	N.A.
V_{eject}	Mortar ejection velocity	m/s	Normal	10	0.833	N.A.	N.A.
m_o	Vehicle initial mass	kg	Normal	10.51	0.35	N.A.	N.A.
V_{winds}	Wind velocity	m/s	Normal	0	5	N.A.	N.A.